Phenolics-rich extract from Agarwood leaf-tea alleviate dextran sulfate sodium (DSS)-induced ulcerative colitis via modulating intestinal barrier function, liver inflammation, and gut microbiota

Ruyan Fan[1*], Wensong Wei[2*], Youjing Wei[1], Xue Lin[1], Shaobo Zhou[4], Lu Wang[1,3#]

1. School of Food Science and Engineering, Hainan University, Haikou 570228, P. R. China;

2. Institute of Food Science and Technology, Chinese Academy of Agricultural Sciences/Key Laboratory of Agricultural Product Processing, Ministry of Agriculture, Beijing 100193, China;

3. Key Laboratory of Food Nutrition and Functional Food of Hainan Province, Hainan University, Haikou 570228, P. R. China;

4. School of Science, Faculty of Engineering and Science, University of Greenwich, Central Avenue, Chatham ME4 4TB, UK

* These authors contributed equally to this article

Corresponding authors:

[#]**Lu Wang,** E-mail: lwang@hainanu.edu.cn; Tel: +86-0898-13367470969; Fax: +86-0898-13367470969; People's Avenue, Meilan District, Haikou, China

Abbreviations

UC (Ulcerative colitis), ALP (Agarwood leaf-tea phenolics-rich extract), NF-κB (Nuclear factor kappa-B), ZO-1 (Zonula Occludens Protein 1), IBD (Inflammatory bowel disease), CD (Crohn's disease), ALT (Agarwood leaf-tea), ELISA (enzyme-linked immunosorbent assay), CON (control group), DSS (dextrose sodium sulfate group), SASP (sulfasalazine group), ALPL (the group fed with a low dose of ALP), ALPH (the group fed with a high dose of ALP), PBS (phosphate buffer solution), DAI (disease activity index), H&E (hematoxylin and eosin), MPO (myeloperoxidase), IL-10 (Interleukin-10), IL-6 (Interleukin-6), IL-1β (Interleukin-1β), TNF-α (tumor necrosis factor-α), INF-γ (Interferon-γ), SDS-PAGE (Sodium dodecyl sulfate-polyacrylamide gel electrophoresis), SCFAS (short-chain fatty acids), GC-MS (Gaschromatography-mass spectrometry), ANOVA (Analysis of Variance), WB (Western Blot), MYD88 (Myeloiddifferentiationfactor88), NF-κB-*p*65 (Nuclear factor kappa-B P65), *p*-NF-κB *p*65 (Phosphorylation nuclear factor kappa-B P65), PCA (Principal Components Analysis), OPLS-DA (Orthogonal Projections to Latent

Structures Discriminant Analysis), KEGG (Kyoto Encyclopedia of Genes and Genomes), LEFSe (Linear discriminant analysis Effect Size), LDA (Linear Discriminant Analysis), JAM (junctional adhesion molecules), LPS (Lipopolysaccharide), TLR (Toll-like receptors), PCOA (Principal co-ordinates analysis), PH (Potential of hydrogen).

Abstract

The increasing incidence of ulcerative colitis (UC) and the side effects of its therapeutic drugs have promoted the search for functional components-derived from natural products as new treatments for UC. In this study, the effect of Agarwood leaf-tea phenolics-rich extracts (ALP) in alleviating dextran sulfate sodium (DSS)-induced UC and its potential mechanism were investigated. The results show that ALP supplementation improved the typical symptoms of UC and decreased pro-inflammatory cytokines. ALP supplementation promoted the expression of tight junction proteins Occludin and ZO-1 on colonic tissues, repaired the intestinal barrier, and relieved further colonic tissues damage. Besides, ALP effectively inhibited the activation of NF-κB signaling pathway and reduced the release of pro-inflammatory cytokines. Moreover, ALP reversed the alteration of gut microbiota in the colitic mice by increasing the abundances of potential beneficial bacteria, e.g. *Parabacteroides*, *Chlamydia*, *Lachnospiraceae*, and decreasing the abundances of potential harmful bacteria, e.g. *Bacteroides* and *Phocaeicola*. The levels of short-chain fatty acids in feces were also regulated by ALP. Furthermore, the correlation analysis suggested that ALP could attenuate DSS-induced UC, which was probably related to the alterations in the gut microbiota. In a short, ALP can ameliorate DSS-induced UC by modulating gut microbiota, intestinal barrier function, and inflammatory responses.

Keywords: Agarwood leaf; ulcerative colitis; intestinal barrier; gut microbiota; NF-κB signaling pathway

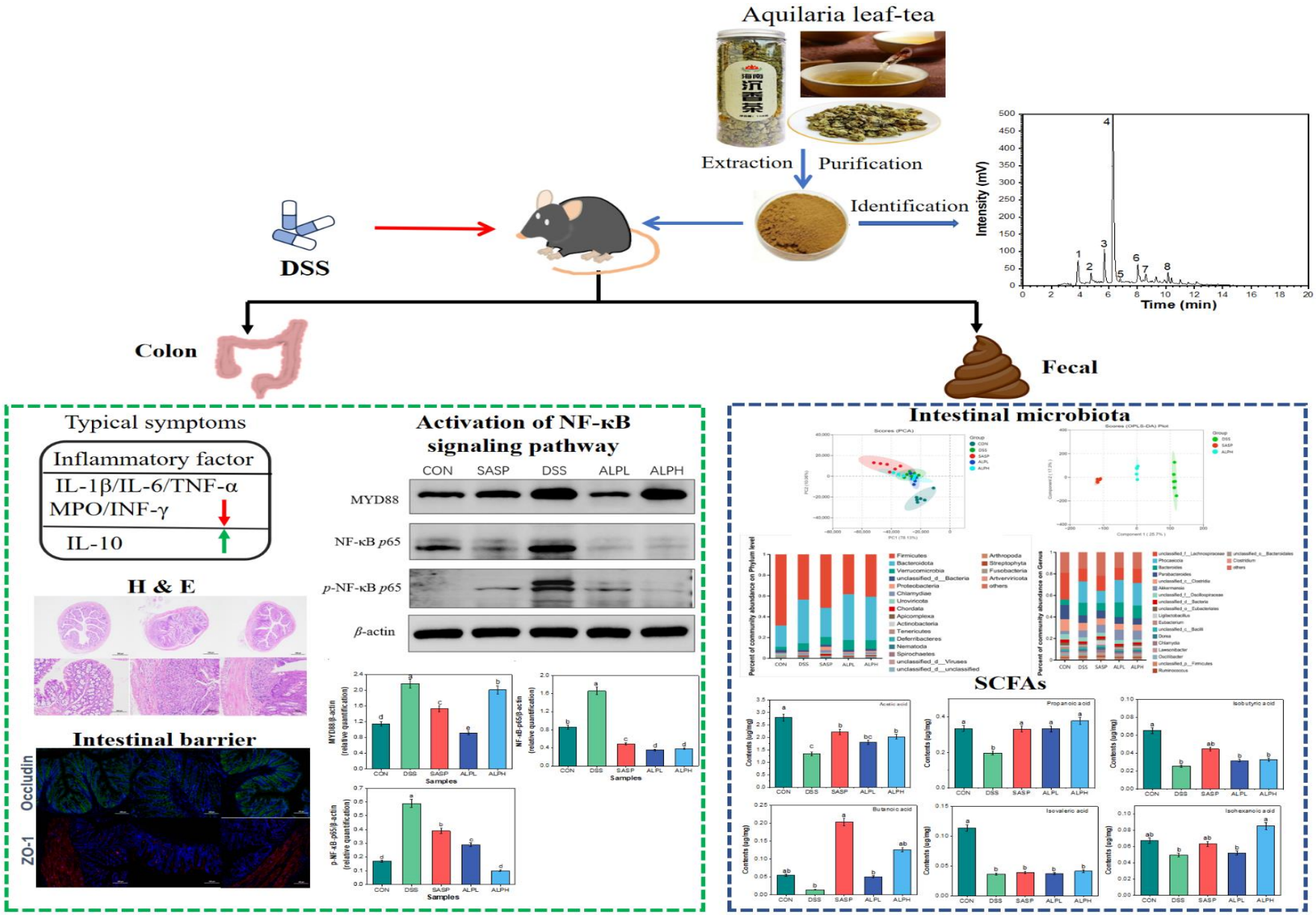
Aquilaria leaf-tea
Extraction
Purification
Identification
DSS
Colon
Fecal
Intensity (mV)
Time (min)
Typical symptoms
Inflammatory factor
IL-1β/IL-6/TNF-α
MPO/INF-γ
IL-10
H & E
Intestinal barrier
Occludin
ZO-1
Activation of NF-κB signaling pathway
CON
SASP
DSS
ALPL
ALPH
MYD88
NF-κB p65
p-NF-κB p65
β-actin
Samples
Intestinal microbiota
SCFAs
Acetic acid
Propanoic acid
Isobutyric acid
Butanoic acid
Isovaleric acid
Isohexanoic acid
Contents (ug/mg)

99

1. Introduction

Inflammatory bowel disease (IBD) is a classical chronic autoimmune disorder that includes Crohn's disease (CD) and ulcerative colitis (UC), characterized by diarrhea and decreased body weight [1]. According to relevant studies, IBD is thought to promote carcinogenesis and increase the risk of cancer [2]. UC is regarded as a chronic immune disease primarily targeting the digestive organs, caused by genetic factors, environmental factors, and intestinal microflora. The pathogenesis of UC is closely related to the expression of tight junction proteins and inflammatory factors. When the expression of tight junction proteins decreases, intestinal tract permeability increases, allowing harmful microorganisms to enter, which ultimately triggers systemic inflammation [3]. Furthermore, pro-inflammatory cytokines produce oxidative products during ulcerative colitis, disrupting the redox balance in the intestinal mucosa and thus exacerbating the inflammation [4]. The incidence of UC is not only high in developed countries but has also increased dramatically in developing countries, making UC a global burden [5]. Currently, drugs such as corticosteroids and immunosuppressants are commonly used in the treatment of UC, but these medications can have detrimental effects on the body [6]. Therefore, the search for natural products to replace drugs in the treatment of UC has become a hot topic.

The use of functional components of natural products for the treatment of various intestinal disorders has been widely accepted as reported in studies [7, 8]. The increasing incidence of UC underscores that phenolics from natural products can effectively reduce and mitigate UC [9]. Many studies have confirmed that polyphenols

122 can effectively relieve inflammatory bowel disease by regulating the intestinal flora
123 [10], and also verified that apple polyphenol extract can alleviate ulcerative colitis by
124 modulating bile acid metabolism and intestinal flora [11-13]. Agarwood (*Aquilaria*
125 *sinensis*) belongs to the Thymeliaceae family, and is mainly distributed in Hainan,
126 Guangdong, Guangxi, Yunnan, and Fujian, etc [14]. Agarwood leaf-tea (ALT) is
127 produced from the leaves of Agarwood (*Aquilaria sinensis*) using the processing
128 technology of red tea. As important local food resources in China, ALT has attracted
129 great interesting due to its wide array of active compounds, including phenolics,
130 flavonoids, polysaccharides, amino acids, and volatile oils [15]. Studies have confirmed
131 that Agarwood leaves extract possesses multiple biological activities, including
132 antioxidant, anti-hypoglycemic, anti-inflammatory, anti-hypolipidemic, anti-arthritic,
133 anti-histamine, anti-tumor, anti-acetylcholinesterase inhibitory, and hepatoprotective
134 effects [16-18]. They have also verified that Agarwood leaves extract may alleviate
135 gastric ulcers by inhibiting oxidation and reducing inflammation. However, the possible
136 potential mechanism of Agarwood leaf-tea phenolics-rich extract (ALP) in alleviating
137 the pathological progression of ulcerative colitis remains unclear.

138 In this study, we investigated the effects of ALP supplementation on symptoms of
139 ulcerative colitis, the expression of tight junction proteins related to the intestinal barrier,
140 and the NF-κB signaling pathway. In addition, this study also analyzed the alteration of
141 gut microbiota and the levels of short-chain fatty acids in the feces of colitic mice
142 following ALP supplementation. A network analysis was conducted to identify
143 relationships between changes in the gut microbiota and metabolic signaling pathway,

144 shedding light on the mechanisms by which ALP alleviates the symptoms of ulcerative
145 colitis in mice.

146 **2. Materials and methods**

147 **2.1. Materials and reagents**

148 Dextrose sulfate sodium (DSS) was purchased from Meron Biotechnology Co., Ltd.
149 (Dalian, China). Sulfasalazine (SASP) was purchased from Yuan Ye Biotechnology Co.,
150 Ltd. (Shanghai, China). Cytokine enzyme-linked immunosorbent assay (ELISA) kits
151 and occult blood kits were purchased from Shanghai Enzyme-linked Biotechnology Co.,
152 Ltd. (Nanjing Jiancheng Bioengineering Institute, Nanjing, China). Agarwood leaf tea
153 was purchased from Hainan Wuzhishan Agricultural Science and Technology
154 Development Co., Ltd. (Hainan, China). Forty male C57BL/6J mice (body weight: 20
155 ± 2 g, age: 7 weeks) were used in the experiment, which was purchased from
156 Guangdong Viton Lihua Laboratory Animal Technology Co., Ltd. (License ID: SCXK
157 2022-0063).

158 **2.2. Extraction, purification and analysis of phenolics from Agarwood leaf-tea**

159 Agarwood leaf tea was freeze-dried, pulverized, and sieved. The extraction and
160 purification of phenolic compounds from the leaf tea were performed according to the
161 previously reported methods [19]. Briefly, the powdered Agarwood leaf tea was mixed
162 with absolute ethanol at a ratio of 1: 10 (*w/v,* g/mL), and then extracted under ultrasound
163 power of 320 W at at 40°C for 30 min. Afterward, the supernatant was concentrated
164 using a rotary evaporator. The purification of phenolic compounds was carried out by
165 a column packed with AB-8 macroporous resin. The purified extracts, rich in phenolics,

were collected via 95% ethanol elution. Finally, the concentrated solutions were freeze-dried to obtain ALP powder. Total phenolic content in ALP was evaluated by using the Folin-Ciocalteu method [20]. The phenolics in ALP power were analyzed by HPLC-Q-Orbitrap-MS/MS and HPLC (high-performance liquid chromatography) method [19].

2.3. Animal experiments

After one week of acclimatization feeding, forty mice at 7 weeks of age were randomly divided into five groups, and each group had eight mice: a control group (CON), a dextrose sodium sulfate group (DSS), a sulfasalazine group (SASP), a group fed with a low dose of Aquilaria leaves phenolic extract (ALPL), and a group fed with a high dose of Aquilaria leaves extract (ALPH). The mice were housed in ventilated cages with four mice per cage. They were all fed standard feed containing the following main nutrients: moisture ≤ 100g/kg, protein ≥ 180g/kg, fat ≥ 40g/kg, fiber ≤ 50g/kg, ash ≤ 80g/kg, and had access to free drinking water. A 12-hour light-dark cycle was maintained, and the temperature was controlled at 24 ± 2°C. From day 1 to day 10, all the mice were given 3.5% (*w/v*) of DSS water to build a model of ulcerative colitis; from day 11 to the end of the experiment, phosphate buffer solution (PBS) was given to the CON and DSS groups, while the three groups of SASP, ALPL, and ALPH were given sulfapyridine (150 mg/kg), low-dose ALP (100 mg/kg) and high dose ALP (200 mg/kg), respectively. Meanwhile, all the above reagents were administered by gavage. The experimental protocol was approved by the Experimental Animal Use and Management Committee of Hainan University (HNUAUCC-2023-00197).

2.4. Typical symptoms analysis of UC

188 According to a previous report, indicators related to inflammation were recorded daily
189 [21]. Subsequently, the disease activity index (DAI) was determined by a
190 comprehensive scoring of body weight, fecal condition, and rectal bleeding. The rectal
191 bleeding evaluation was performed using an occult blood kit (Nanjing Jiancheng
192 Bioengineering Institute, Nanjing, China), with the scoring criteria shown in Table S1.

193 **2.5. Histopathological analysis**

194 Approximately 1 cm of undamaged colon tissue was fixed in 4% paraformaldehyde.
195 This was followed by trimming, dehydration, embedding, sectioning, and hematoxylin
196 and eosin (H&E) staining. After sealing, the colon tissue sections were observed under
197 an orthotropic white light photomicrograph (Eclipse Ci-L) at 40× and 200×
198 magnifications. The accuracy of histopathological analysis is shown in Table S2.

199 **2.6. Colon biochemical analysis**

200 The distal colon was placed in PBS and separated by high-speed centrifuge at 1000 rpm
201 for 10 min at 4°C to obtain the supernatant, which was then used for the determination
202 of biochemical indexes. The supernatant was assayed for MPO (Myeloperoxidase), IL-
203 6 (Interleukin-6), IL-10 (Interleukin-10), IL-1β (Interleukin-1β), TNF-α (Tumor
204 necrosis factor-α), and INF-γ (Interferon-γ) using the kit (Nanjing Jiancheng
205 Bioengineering Research Institute, Nanjing, China). The concentration of the standard
206 curve was determined according to the kit manufacturer's instructions, which was then
207 used to calculate the levels of biochemical indicators.

208 **2.7. Western blotting**

209 The tissue blocks were washed 2-3 times with pre-cooled PBS to remove blood stains,

then cut into small pieces, and placed in homogenizing tubes. Two 4-mm homogenizing beads were added, along with 10 times the volume of tissue in lysate containing various protease inhibitors, which were added a few minutes before use. The homogenization program was established and once completed, the homogenized tube was removed and placed on ice with the lysate for 30 minutes, with shaking every 5 minutes to ensure that the tissue was completely dissolved. Afterward, the samples were centrifuged at 12,000 rpm and 4°C for 10 minutes to collect the supernatant, which is the total protein solution. This protein solution was then mixed with reduced protein up-sampling buffer in a 4:1 ratio, denatured in a boiling water bath for 15 minutes, and stored at -20°C for later use. Subsequent procedures included SDS-PAGE electrophoresis, transfer, immunoreactivity, and chemiluminescence. Finally, the data were analyzed using AIWBwell^{TM} analysis software.

2.8. Gut microbiota analysis

After completing the DNA extraction of the samples, the PE libraries were composed using NEXTFLEX™ Rapid DNA-Seq kits according to the manufacturer's instructions, and then the amplifiers were sequenced using Illumina NovaSeq Reagent Kits according to the instructions. Optimization processes such as splitting, quality shearing, and removal of contamination were performed on the original sequences. The optimized sequence was then used to assemble and predict genes, which were subsequently classified by species and function. Following these steps, statistical analyses including similarity clustering, group ordering, and difference comparison were conducted. Further analyses of α-diversity, β-diversity, species composition, and

232 species with significant differences were conducted using the Majorbio Cloud Platform
233 (https://cloud.majorbio.com).

234 **2.9. Determination of contents of short-chain fatty acids (SCFAs)**

235 20 mg of colonic content was weighed into a 2 mL grinding tube and 800 μL of 0.5%
236 PBS was added. The sample was then frozen and ground for 3 minutes sonicated for 10
237 minutes, and centrifuged at 4°C and 13,000 rpm for 15 minutes. N-butanol was added
238 to the supernatant for solvent extraction, the mixture was vortexed for 10 seconds,
239 sonicated again for 10 minutes, and centrifuged at 4°C and 13,000 rpm for 5 minutes.
240 The clear supernatant was then transferred into an injection vial. The analysis was
241 performed using an 8890B-7000D GC/MSD gas chromatograph (Agilent Technologies
242 Inc., CA, USA). Target short-chain fatty acids were automatically identified and
243 quantified using MassHunter quantitative software (Agilent), with manual verification.
244 The detected concentrations were calculated from the standard curve and converted to
245 the actual content of short-chain fatty acids in the sample. This quantification method
246 using GC-MS (Gas chromatography-mass spectrometry) had been employed in
247 previous research [22].

248 **2.10. Statistical analysis**

249 Data were statistically analyzed by one-way ANOVA (Analysis of Variance) and
250 Duncan's post-hoc test using IBM SPSS Statistics 27 software and the results were
251 expressed as mean ± standard deviation. Graphs were plotted using Origin 2019b
252 software. Values of $p < 0.05$ indicate statistically significant differences.

253 **3. Results**

3.1. Effects of ALP supplementation on typical symptoms in DSS-induced UC mice

Total phenolic content in ALP was evaluated using the Folin-Ciocalteu method, which was 56.24 ± 1.43%. In addition, the contents of sugar, water, and protein in ALP were 7.21 ± 0.59%, 9.13 ± 0.42%, and 5.49 ± 1.21%, respectively, along with unknown ingredients. UPLC-TOF/MS and HPLC method results showed that the representative phenolic compounds in ALP included cyanidin-3,5-O-diglucoside (58.53 ± 2.03 mg/g), malvidin-3-glucoside (34.16 ± 2.91 mg/g), epicatechin (74.51 ± 7.71 mg/g), EGCG (Kyoto Encyclopedia of Genes and Genomes, 98.96 ± 1.86 mg/g), dihydromyricetin (17.65 ± 1.68 mg/g) and astragalin (41.78 ± 0.45 mg/g) (Fig. 1A and B). Fig. 2A-E shows the typical symptoms and the DAI index of ALP supplementation on DSS-induced UC mice. During the first 10 days, all groups except the CON group experienced decreases in body weight, water intake, and food intake. After supplementation with ALP, the SASP, ALPL, and ALPH groups regained their body weights, which essentially recovered to levels comparable to those of the CON group after 10 days of treatment. During the modeling period, drinking water and food intake decreased in all groups except for the CON group. However, these levels recovered after the treatment. In terms of the disease indicator DAI, the DSS group showed higher scores. However, the scores decreased in the SASP, ALPL, and ALPH groups after treatment. Both ALPL and ALPH groups recovered to levels comparable to the SASP group (Fig. 2B). As shown in Fig. 2C, the percentages of liver, spleen, and kidney weights in the DSS group were higher than those in the other four groups; however, there was no significant difference among the remaining four groups. The colon length

in the DSS group was significantly shorter than that of the other four groups. Additionally, the colon in the DSS group was noticeably thicker compared to those in the remaining groups (Fig. 2D and E). In conclusion, the recovery effect of the two ALP-treated groups was comparable to that of the SASP-treated group, and both had a restorative effect on DSS-induced UC.

3.2. Effects of ALP supplementation on biochemical parameters in DSS-induced UC mice

Changes in inflammatory factors in the colon can evaluate the degree of damage, and as shown in Fig. 3A-F, levels of the pro-inflammatory factors IL-1β, IL-6, TNF-α, INF-γ, and MPO increased in the DSS group compared with the CON group. Conversely, the anti-inflammatory factor IL-10 decreased. This trend was to opposite in the remaining three groups. There were no significant differences in the levels of pro-inflammatory factors IL-6, INF-γ, and MPO, and the anti-inflammatory factor IL-10, between the ALP-treated groups and the SASP group. Similarly, there were no significant differences in IL-1β levels between the ALPH and SASP groups, nor TNF-α levels between the ALPL and SASP groups. In conclusion, the effects of the ALP-treated groups were comparable to those of the SASP-treated group, and all had a restorative effect on DSS-induced UC.

3.3. Effect of ALP supplementation on tissue morphology and colon mRNA expression in DSS-induced UC mice

H&E staining was performed on the colonic tissues, with the section results shown in Fig. 4A. The intestinal tissues of the CON group exhibited clear structural layers with

298 distinct demarcation. The mucosa surface was intact, and due to the shape and structure
299 of the cells, the distribution of intestinal glands in the lamina propria was rich and
300 regular, featuring numerous goblet cells. The muscle layer was uniformly stained, and
301 the myofibrils appeared normal with a regular arrangement. There was no significant
302 inflammation. In the DSS group, a large area of ulcer was observed in the intestinal
303 tissue. The mucosal epithelium at the site of injury was detached, and a large number
304 of intestinal glands had undergone necrosis and were replaced by hyperplastic
305 connective tissues, indicated by black arrows. The injury extended to the plasma
306 membrane, with blood vessels penetrating it, and significant infiltration of granulocytes
307 and lymphocytes was noted in each layer, as marked by red arrows. In contrast, the
308 intestinal tissues of the SASP group showed focal erosion with an intact intestinal
309 epithelial structure. A small number of intestinal glands were replaced by hyperplastic
310 connective tissues, as indicated by black arrowheads. There was also punctate
311 infiltration of lymphocytes, shown with red arrowheads, and a localized sparse
312 arrangement of myocytes in the muscularis propria, marked by blue arrowheads. In the
313 ALPL group, the intestinal tissue displayed focal ulceration with an intact mucosal
314 epithelial structure. A small number of intestinal glands were necrotic and replaced by
315 hyperplastic connective tissues, indicated by black arrows. The damage extended into
316 the submucosal layer, with minor infiltration of granulocytes and lymphocytes in the
317 lamina propria and submucosal layer, marked by red arrows. Some intestinal glands
318 had irregular shapes and occasional dilatation, shown by yellow arrows. In the ALPH
319 group, the intestinal tissues exhibited focal erosions with an intact mucosal epithelial

structure, and a small number of necrotic intestinal glands were replaced by hyperplastic connective tissues, indicated by black arrows, alongside punctate infiltration of lymphocytes, shown by red arrowheads. Pathological analysis of the colon tissues revealed that the scores for the DSS group were significantly different from those of the CON group, while there were no significant differences observed among the other groups (Fig. 4C).

As shown in Fig. 4B, the immunofluorescent proteins ZO-1 and occludin in colon tissues were photographed. Compared to the CON group, the expression levels of these proteins were decreased in the DSS group. After treatment, their expression increased in both the ALPL and ALPH groups. Surface densitometry was performed for these proteins, with results displayed in Fig. 4D and E. The surface densities of ZO-1 and occludin were lower in the DSS group compared to the other four groups. No significant differences in protein expression density were found among the SASP, ALPL, and ALPH groups. In summary, ALP treatment had a restorative effect on DSS-induced UC.

3.4. Effect of ALP on NF-κB signaling pathway in mice with DSS-induced UC

Activation of the NF-κB pathway is strongly associated with ulcerative colitis, as demonstrated and exacerbated in previous studies [23, 24]. This experiment measured MYD88, NF-κB *p*65, and *p*-NF-κB *p*65 on the NF-κB pathway through western blotting, as shown in Fig. 5A. The relative content of these proteins to β-actin was calculated. As shown in Fig. 5B-D, compared with the CON group, the DSS group showed significant increases in MYD88, NF-κB *p*65, and *p*-NF-κB *p*65, while the SASP group and ALP treatment group showed a significant decrease in protein levels.

342 Especially, the expression levels of NF-κB *p*65 and *p*-NF-κB *p*65 were even lower than
343 those in the CON group. The protein expression levels in the ALP treatment group were
344 comparable to those in the SASP group. Additionally, the inhibitory effects on *p*-NF-
345 κB *p*65 in both the ALPL and ALPH groups occurred in a dose-dependent manner.
346 These results showed that ALP can inhibit the activation of the NF-κB pathway by
347 inhibiting the expression of MYD88, NF-κB *p*65, and *p*-NF-κB *p*65, thus alleviating
348 ulcerative colitis.

349 **3.5. Effect of ALP supplementation on gut microbiota in ulcerative colitis mice**

350 There was a significant decrease in the Sobs, Ace, Chao, and Simpson indices in the
351 DSS group compared to the CON group. Conversely, there was a significant rebound
352 in the Sobs, Ace, Chao, and Shannon indices in the SASP, ALPL, and ALPH groups.
353 However, no significant differences were found in the Simpson indices between the
354 SASP, ALPL, and ALPH groups (Table S3). Based on the Bray Curtis distance
355 algorithm for data processing, a significant difference in PCA (Principal Components
356 Analysis) results was observed between the CON group and the other four modeling
357 groups (Fig. 6A), while the positive control group SASP was closer to the other three
358 groups. Therefore, 0PLS-DA (Orthogonal Projections to Latent Structures Discriminant
359 Analysis) analysis was performed on DSS, SASP, and ALPH, in which a significant
360 difference in scores was observed among the three groups (Fig. 6B). Further KEGG
361 (Kyoto Encyclopedia of Genes and Genomes) functional enrichment analysis was
362 conducted on the ALPH and DSS groups, focusing on the top 20 enriched groups (Fig.
363 6C). The results indicated that KEGG pathways were significantly different in the DSS

364 group compared to the ALPH group. The DSS group was mainly enriched in
365 Peptidoglycan biosynthesis, Malaria, Nicotinate and nicotinamide metabolism, Fatty
366 acid biosynthesis, etc., while the ALPH group was mainly enriched in
367 Lipopolysaccharide biosynthesis, Biosynthesis of secondary metabolites, Valine,
368 leucine, and isoleucine. Enrichment of ine biosynthesis, Photosynthesis, etc. LEfSe
369 (Linear discriminant analysis Effect Size) differential discriminant analysis was carried
370 out to estimate the impact of each component abundance on differential effects, in
371 which the LDA (Linear Discriminant Analysis) threshold was adjusted to be greater
372 than 3.5 to obtain the LDA index (Fig. 6D). The higher LDA score, the more significant
373 the effect of species abundance on the difference. It was observed that the LDA value
374 of Dorea in the SASP group was around 4, Bacteroides in the ALPL group was generally
375 above 3, and Phocaeicola LDA in the ALPH group reached 5. Finally, significant
376 differences in microorganisms were analyzed among the five groups, and results
377 showed that there were 15 microorganisms with significance (Fig. 6E).

378 Community abundance of intestinal flora was analyzed at the phylum level, as
379 shown in Fig. 7A, the phylum with community relative abundance greater than 1%
380 among the five groups included Firmicutes, Bacteroidota, Verrucomicrobia,
381 unclassifed-d-Bacteria, Proteobacteria, Chlamydiae, Uroviricota, and Chordata.
382 Compared to the CON group, the abundance of Firmicutes and unclassified-d-Bacteria
383 was significantly lower in the remaining four groups, while the abundance of
384 Bacteroidota was significantly higher, especially in the DSS group, where it was
385 regulated in a dose-dependent manner. There was no significant difference between the

ALPL and ALPH groups in the abundance of Firmicutes (Fig. 7C). At the genus level, as shown in Fig. 7B, compared to the CON group, the remaining four groups exhibited a significant decrease in the abundance of *unclassified-f-Lachnospiraceae*, *Parabacteroides*, and *unclassified-c-Clostridia*. Conversely, the abundance of *Phocaeicola*, *Bacteroides*, and *Akkermansia* was significantly increased. There were no significant differences in genus-level abundance between the ALPL and ALPH groups, which were regulated in a dose-dependent manner.

The species with significant differences in all groups were analyzed, with the results shown in Fig. 7D. The species with significantly different abundance in different groups include *Phocaeicola, Bacteroides, Akkermansia, unclassified-f-Oscillospiraceae, Dorea, unclassified-o-Bacteroidales, Clostridium, unclassified-f-Bacteroidaceae, Parasutterella, Acutalibacter, Acetatifactor, Anaerotruncus, Hungatella, Enterocloster, unclassified-f-Peptococcaceae*. Compared to the CON group, the abundances of *Parabacteroides, Lachnospiraceae, Chlamydia*, and *Dorea* were increased in the remaining four groups. Aside from that, there were no significant differences in species abundance between the ALPL and ALPH groups, which were regulated in a dose-dependent manner. In summary, ALP treatment can alter the composition of intestinal communities in DSS-induced conditions.

3.6. Effect of ALP supplementation on the levels of SCFAs in ulcerative colitis mice

As shown in Fig. 8A-F, compared with the CON group, the levels of acetic acid, propionic acid, butanoic acid, isobutyric acid, isovaleric acid, and isohexanoic acid in the DSS group were significantly reduced. Except for isovaleric acid, the levels of the

other acids (acetic, propionic, isobutyric, butanoic, and isohexanoic) were significantly different in the DSS group compared to the other four groups. There was no significant difference in the levels of acetic acid, propionic acid, butanoic acid, isobutyric acid, isovaleric acid, and isohexanoic acid among the SASP, ALPL, and ALPH groups, and there was a significant increase in the content of isohexanoic acid in ALPH. The CON group had the highest total short-chain fatty acid content, while the DSS group had the lowest total short-chain fatty acid content, the two groups showed a significant difference. The total short-chain fatty acid content in the SASP, ALPL, and ALPH groups was comparable and significantly higher than that of the DSS group (Fig. 8G). In conclusion, ALP treatment can modulate short-chain fatty acids in a dose-dependent manner and has beneficial effects on DSS-induced UC mice.

3.7. Correlation between intestinal microbiota and DSS-induced UC-related indices

To further investigate the possible association of gut microbiota with colitis, inflammatory factors, intestinal permeability indices, tight junction proteins, and SCFA (short-chain fatty acids) were analyzed with Spearman correlation heat maps (Fig. 9). At the Phylum level, Firmicutes has a significant positive correlation with most SCFAs, tight junction proteins, IL-10, and total SCFAs, but has a significant negative correlation with colonic pathological analysis and Valeric acid ($p < 0.05$). But Bacteroidota correlates with these indexes exactly opposite to Firmicutes. At the genus level, *Lachnospiraceae* and *Parabacteroides* show similar trends in correlation, they were positively correlated with the remaining SCFAs, total SCFAs, colon pathological

analysis, IL-10, and tight junction proteins, except for Valeric acid, which was negatively correlated. In addition, *Phocaeicola, Bacteroides,* and *Akkermansia* correlations showed similar trends. They were negatively correlated with the rest of the previously mentioned indicators except for a positive correlation with Valeric acid and colon pathological analysis. In particular, the correlation between gut microbiota and NF-κB pathway-expressed proteins was not significant.

4. Discussions

Since the publication of a new method for inducing ulcerative colitis in Gastroenterology in the 20th century, a model of ulcerative colitis stimulated with DSS has mimicked the pathological damage and symptoms of human UC [25]. This method has then been used to study the pathogenesis and pharmacodynamics of UC [26]. Currently, there are two main modeling methods for UC: one involves consuming DSS water for about a week to establish acute colitis, while the other employs periodic consumption of DSS water to induce chronic colitis. Although the degrees of modeling differ, it has been shown that DSS-induced acute and chronic colitis exhibit similar symptoms and histopathological changes, and the changes in the intestinal flora of the acute colitis model more closely resemble those observed in ulcerative colitis [27]. In addition, acute colitis is not only a shorter modeling and treatment cycle but also a highly manipulative experiment [28]. Therefore, this experiment was conducted using 3.5% DSS for drinking for 10 days, resulting in an acute colitis model. The results of this study showed that ALP effectively attenuated the symptoms and intestinal inflammation of DSS-induced colitis in mice, regulated the intestinal flora and SCFA

452 levels, and, at the same time, increased the expression levels of tight junction proteins.

453 DSS-induced UC is mainly characterized by diarrhea, blood in the stool, decreased
454 water and food intake, weight loss, shortened colon length, and thickening of the colon
455 [29]. The results of the present study showed that ALP significantly improved the above
456 pathologic features in mice with DSS-induced ulcerative colitis. In particular, at the late
457 stage of ALP treatment, the water intake of mice in the SASP, ALPL, and ALPH groups
458 increased to different degrees, but the fluctuation of water intake was again large.
459 Because all the mice were relieved of their symptoms and their mental state gradually
460 improved in the later stages of the treatment, thus leading to an increase in the
461 fluctuation of water intake, but the exact reason for this needs to be confirmed by more
462 in-depth studies. In addition, there was an interesting finding on the DAI index, which
463 decreased in the DSS group at the later stage of treatment, suggesting a potential self-
464 healing function in acute colitis. This is supported by related studies, which
465 demonstrated that the DSS-induced UC mouse model can self-repair by regulating
466 disorganized intestinal flora [30]. Furthermore, liver, spleen, and kidney indices were
467 significantly higher in the DSS group compared to the CON group. Research indicates
468 that the body undergoes an inflammatory response during which capillary dilation,
469 blood vessel filling, and increased vessel permeability occur, leading to swelling as
470 leukocytes and proteins accumulate locally [31]. However, ALP treatment effectively
471 relieved the swelling of the spleen and other organs caused by DSS, mirroring its effect
472 on colon symptoms such as shortening and thickening.

473 An abnormal structure of tight junction proteins in intestinal epithelial cells is one

of the key factors causing damage to the UC intestinal barrier [32]. The intact monolayer of intestinal epithelial cells protects the official lumen from pathogens and toxic substances. Additionally, the tightly connected epithelial cells in intestinal tissues maintain the intestinal barrier and regulate the permeability of ions, nutrients, and water [33]. A tight junction is a complex composed of many proteins, including occludin, prefibrillar, claudins, and junctional adhesion (JAM) [32]. We determined the major proteins in tight junction proteins (ZO-1 and oculudin) and found that ALP treatment could effectively alleviate the reduction of protein expression levels caused by DSS, and the effect was even comparable to that of SASP. This finding is consistent with a study by Chen et al, [34] which showed that natural cordyceps polysaccharides alleviated DSS-induced colitis in mice.

Relevant studies have shown that the levels of inflammatory factors are closely associated with UC. Pro-inflammatory factors include TNF-α, IL-6, IL-1β, and anti-inflammatory factors mainly include IL-10. TNF-α promotes the proliferation and differentiation of T cells and exacerbates intestinal inflammation [35, 36]. IL-1β is involved in the aggregation of leukocytes in inflamed tissues and activates innate immune lymphocytes [37]. Additionally, IL-6 activates the NF-κB pathway to modulate DSS-induced colitis in mice [38]. According to the KEGG database, pathways associated with UC mainly involve the interaction of NF-κB peptidoglycan and LPS (Lipopolysaccharide) with TLR (Toll-like receptors) family. This interaction activates the NF-κB, which is regulated by the DNA for the expression of TNF-α, known to increase intestinal inflammation. On the other hand, inflammatory factors enter the cell

to activate MYD88, then further activate NF-κB *p*65. After phosphorylation, NF-κB *p*65 activates the NF-κB pathway, controlling the release of pro-inflammatory factors and INF-γ, which can indirectly cause colonic tissue injury. Studies on colitis models have demonstrated that SASP, as an NF-κB inhibitor, can effectively improve UC [39]. To explore the related mechanisms, inflammatory factors related to the NF-κB pathway were measured and Western Blot (WB) validation was performed. The results revealed that ALP treatment could inhibit the NF-κB pathway and block the downstream response by suppressing the phosphorylation level of NF-κB *p*65, which in turn effectively decreased IL-6, IL-1β, TNF-α, INF-γ, and MPO, and effectively increased the anti-inflammatory factor IL-10, thus alleviating UC.

Currently, a consensus has been reached regarding the gut microbiota and its metabolites as having a significant impact on IBD. The development of colitis usually leads to a decrease in the diversity and abundance of the gut microbiota [40-42]. This experiment demonstrates that ALP can alleviate DSS-induced UC mice by modulating gut flora, including increasing species richness and species diversity. This result has also been confirmed in related studies [43]. The generally accepted theory is that the gut microbiota, which remains relatively stable at the phylum level, is predominantly composed of Firmicutes, Bacteroidota, Verrucomicrobia, Actinobacteriota, and Desulfobacterota. At the level of the phylum, Firmicutes and Bacteroidota have been widely studied because they act as dominant phyla in the gut. It is widely accepted that the ratio of F/B is strongly associated with IBD. Furthermore, it is generally acknowledged that this ratio in IBD-afflicted mice is significantly lower than in normal

518 mice [44, 45]. This was also evident in our experiments, with this ratio being
519 significantly lower in the DSS group than in the CON group. It can be hypothesized
520 that ALP attenuates DSS-induced acute colitis by modulating the abundance of
521 Firmicutes and Bacteroidota. At the genus level, the functions of individual bacteria
522 were further analyzed. *Lachnospiraceae*, a beneficial bacterium, has been found to have
523 its growth inhibited in DSS environments, while therapeutic drugs promote its growth
524 [39, 46]. This is exactly what was presented in this experiment, with the CON group
525 having the best abundance, the DSS group having a significantly lower abundance, and
526 the ALP-treated groups showing a dose-dependent phenomenon. *Bacteroides*, which
527 are pathogenic or conditionally pathogenic bacteria in the gut with a high survival rate
528 at higher pH values, can further contribute to inflammation when they proliferate or
529 when the homeostasis of the body is upset [47, 48]. In this experiment, the CON and
530 SASP groups had the lowest abundance of *Bacteroides*, while the DSS group had a
531 higher abundance, and decreased in a dose-dependent manner in the ALPL and ALPH
532 groups. In addition, *Bacteroides* were negatively correlated with SCFAs and positively
533 correlated with pro-inflammatory factors, and the increase in SCFAs in the ALP-treated
534 groups led to a decrease in pH, a decrease in *Bacteroides* survival, and a decrease in
535 pro-inflammatory factor levels, resulting in the alleviation of DSS-induced colitis
536 symptoms. In particular, we found that *Phocaeicola* was essentially absent in the CON
537 group, but was present in all four groups induced by DSS, and after SASP and ALP
538 treatments, the SASP group had the lowest abundance of *Phocaeicola*, and the ALP-
539 treated groups showed a dose dependence. This may bacause DSS-induced UC

produced in mice creates a favorable environment for the growth of *Phocaeicola*. Based on the above account, it is speculated that ALP attenuates DSS-induced UC supposedly by decreasing pH by increasing the content of SCFAs to achieve resistance to the increase in *Bacteroides*.

A growing number of studies are now reporting that SCFAs-producing gut microbes can take different approaches to alleviate colitis. Such as *Akkermansia, Dubosiella, Lachnospiraceae, unclassified _ Oscillospiraceae, Colidextribacter,* and *Faecalibaculum* [49]. The most important roles of SCFAs in the body's inflammatory response are to promote intestinal epithelial cell differentiation and mucin secretion, and to regulate inflammation by inhibiting cytokine production by immune cells via the histone deacetylase pathway [50]. Akkermansia is mainly used to degrade mucins in the degraded intestinal mucus layer and produce propionic acid, which then stimulates cuprocyte differentiation to maintain the integrity of the mucosal barrier [51]. In this experiment, *Akkermansia* was negatively correlated with propanoic acid and tight junction proteins, and positively correlated with colon pathological analysis, after ALP treatment, propanoic acid levels increased in the ALP-treated groups, with a consequent decrease in the level of *Akkermansia*, and then an increase in colon tight junction proteins, which maintains the intestinal integrity of the colonic tissue. *Lachnospiraceae* are key beneficial bacteria in the gut microbiota. *Lachnospiraceae* was positively correlated with SCFAs, and tight junction proteins, and negatively correlated with colonic pathological analyses and pro-inflammatory factors. After ALP treatment, the ALP-treated groups showed an increase in SCFAs and tight junction proteins, a

562 subsequent increase in *Lachnospiraceae* abundance, a decrease in cellular
563 inflammatory factors, and a remission of DSS-induced colonic symptoms.

564 Based on the above discussion, we hypothesize possible mechanisms by which
565 ALP alleviates DSS-induced UC. ALP may restore gut microenvironmental
566 homeostasis by modulating the diversity and abundance of the gut microbiota. Not only
567 does ALP have a significant impact on the composition of short-chain fatty acids, but
568 SCFAs are also known to aid in repairing the intestinal barrier and modulating
569 inflammatory factors. On the other hand, a relatively intact intestinal barrier can resist
570 external pathogens and toxic substances from disrupting the body's homeostasis.
571 Consequently, the MYD88/NF-κB signaling pathway is inhibited, and the release of
572 inflammatory factors is further reduced, thus mitigating the risk of a vicious cycle of
573 colon inflammation.

574 **5. Conclusions**

575 In conclusion, our experiments demonstrated for the first time the alleviating effect of
576 ALP on DSS-induced UC in mice and explored the possible underlying mechanisms.
577 The results showed that ALP ameliorated colonic disorders such as blood in stool,
578 shortened colon, thickened colon, and elevated DAI. In addition, ALP can inhibit the
579 expression of the MYD88/NF-κB inflammatory signaling pathway and reduce the
580 production of pro-inflammatory cytokines such as TNF-α, IL-6, and IL-1β. On the other
581 hand, ALP effectively alleviated the expression of tight junction proteins (ZO-1 and
582 Occludin) and repaired the intestinal barrier function to some extent. In addition, ALP
583 modulated the DSS-induced dysbiosis of intestinal flora and contributed to some extent

584 to the changes in SCFAs. Overall, ALP can ameliorate DSS-induced ulcerative colitis
585 by regulating inflammation and intestinal barrier, regulating the disordered intestinal
586 flora, increasing the level of SCFAs, and synergistically re-establishing intestinal
587 homeostasis to further restore intestinal barrier function and alleviate inflammation.
588 This study provides a theoretical basis and a reference value of research on the
589 prevention of UC by ALP.

590 **Author Contributions**

591 **Ruyan Fan** and **Wensong Wei:** Methodology, Investigation, Data analysis, Wrote the
592 original draft; **Youjing Wei:** Resources and Investigation, Data analysis and Data
593 curation; **Shaobo Zhou** and **Xue Lin:** Data curation and Review & Editing; **Lu Wang:**
594 Supervision, Funding, Data curation and Reviewing & Editing

595 **Acknowledgments**

596 The study was supported by the National Natural Science Foundation of China (No.
597 32360109 and No. 32201991), the Hainan Province Science and Technology Special
598 Fund, China (No. ZDYF2022SHFZ052), and the Collaborative Innovation Center
599 project of Hainan University, China (No. XTCX2022NYC19).

600 **Conflict of interest**

601 The authors declare no competing financial interest.

602 **References**

603 [1] Y. J. Wang, Q. M. Li, X. Q. Zha, J. P. Luo, *Food Funct.* **2022**, *13*, 143.
604 [2] B. Khor, A. Gardet, R. J. Xavier, *Nature* **2011**, *474*, 307.
605 [3] H. Ge, T. Li, Q. Yang, Y. Tang, J. Liu, Y. Yu, T. Zhang, *Food Frontiers* **2023**, *4*, 782.
606 [4] G. P. Ramos, K. A. Papadakis, *Mayo Clin. Proc.* **2019**, *94*, 155.

[5] *Nat. Rev. Dis. Primers* **2020**, *6*, 73.
[6] M. H. G. Foppen, E. A. Rozeman, S. van Wilpe, C. Postma, P. Snaebjornsson, J. V. van Thienen, M. E. van Leerdam, M. van den Heuvel, C. U. Blank, J. van Dieren, J. B. A. G. Haanen, *Esmo Open* **2018**, *3*.
[7] P. Lu, J. Chen, Y. Chen, X. Quan, J. Liu, Y. Han, Y. Li, L. Yang, J. B. Wan, Y. Zhao, *Food Frontiers* **2023**, *4*, 2081.
[8] M. Caban, U. Lewandowska, *J. Funct. Foods* **2022**, *95*.
[9] Y. Mi, W. Zhang, H. Tian, R. Li, S. Huang, X. Li, G. Qi, X. Liu, *Food Funct.* **2018**, *9*, 1510.
[10] L. Yang, Y. Gao, M. A. Farag, J. Gong, Q. Su, H. Cao, W. Zhang, Y. Zhao, H. Wang, *Food Frontiers* **2023**, *4*, 1794.
[11] F. Li, H. Yan, L. Jiang, J. Zhao, X. Lei, J. Ming, *Foods* **2022**, *11*.
[12] H. Li, L. M. Christman, R. Li, L. Gu, *Food Funct.* **2020**, *11*, 4878.
[13] F. Liu, X. Wang, D. Li, Y. Cui, X. Li, *Phytother. Res.* **2021**, *35*, 1468.
[14] Y. Wu, C. Liu, H. F. Li, J. B. Sun, Y. Y. Li, W. Gu, D. Y. Wang, J. G. Liu, Y. L. Hu, *Biochem. Syst. Ecol.* **2014**, *55*, 41.
[15] R. Wang, R. He, Z. Li, S. Li, C. Li, L. Wang, *Sep. Purif. Technol.* **2021**, *275*.
[16] A. Z. Adam, S. Y. Lee, R. Mohamed, *J. Herb. Med.* **2017**, *10*, 37.
[17] M. A. Eissa, Y. Z. H. Y. Hashim, M. H. Mohd Nasir, Y. A. Nor, H. M. Salleh, M. L. M. Isa, S. S. S. Abd-Azziz, N. M. Abd Warif, E. Ramadan, N. M. Badawi, *Drug Deliv.* **2021**, *28*, 2618.
[18] C. Wang, D. Peng, Y. Liu, Y. Wu, P. Guo, J. Wei, *Evid-based Comp. Alt. Med.* **2021**, *2021*.
[19] Y. Qin, R. Fan, Y. Liu, S. Qiu, L. Wang, *Food Funct.* **2023**, *14*, 9295.
[20] R. Y. Fan, S. J. Li, Y. J. Wei, Y. X. Liu, L. Wang, *Food Sci. Hum. Well.* **2024**.
[21] Q. Li, W. Wu, X. Fang, H. Chen, Y. Han, R. Liu, B. Niu, H. Gao, *Food Chem.* **2022**, *387*.
[22] S. Zhang, Y. Sun, Q. Nie, J. Hu, Y. Li, Z. Shi, H. Ji, H. Zhang, M. Zhao, C. Chen, S. Nie, *Carbohyd. Polym.* **2024**, *323*.
[23] X. Zhang, Y. Zhou, M. S. Cheong, H. Khan, C. C. Ruan, M. Fu, J. Xiao, W. S.

637 Cheang, *Food Frontiers* **2022**, *3*, 785.
638 [24] J. Xin, *Digest. Liver Dis.* **2023**, *55*, 169.
639 [25] I. Okayasu, S. Hatakeyama, M. Yamada, T. Ohkusa, Y. Inagaki, R. Nakaya,
640 *Gastroenterology* **1990**, *98*, 694.
641 [26] P. K. Randhawa, K. Singh, N. Singh, A. S. Jaggi, *Korean J. Physiol. Pha.* **2014**,
642 *18*, 279.
643 [27] H. M. Xu, H. L. Huang, Y. D. Liu, J. Q. Zhu, Y. L. Zhou, H. T. Chen, J. Xu, H. L.
644 Zhao, X. Guo, W. Shi, Y. Q. Nie, Y. J. Zhou, *Bmc Microbiol.* **2021**, *21*.
645 [28] J. Bilsborough, M. F. Fiorino, B. W. Henkle, *Expert Opin. Drug Dis.* **2021**, *16*, 567.
646 [29] Y. Shang, Z. Zhai, J. Huang, L. Li, X. Zuo, *Biotechnol. Biotec. Eq.* **2022**, *36*, 200.
647 [30] J. Liu, Y. Gao, J. Zhou, X. Tang, P. Wang, L. Shen, S. Chen, *Life Sci.* **2020**, *263*.
648 [31] P. Wang, M. Cai, K. Yang, P. Sun, J. Xu, Z. Li, B. Tian, *J. Agri. Food Chem.* **2023**,
649 *71*, 16630.
650 [32] K. L. Edelblum, J. R. Turner, *Curr. Opin. Pharmacol.* **2009**, *9*, 715.
651 [33] J. R. Turner, *Am. J. Pathol.* **2006**, *169*, 1901.
652 [34] S. Chen, J. Wang, N. Dong, Q. Fang, Y. Zhang, C. Chen, S. W. W. Cui, S. Nie,
653 *Food Funct.* **2023**, *14*, 720.
654 [35] T. Y. Yu, Y. M. Feng, W. S. Kong, S. N. Li, X. J. Sun, G. Zhou, R. F. Xie, X. Zhou,
655 *Front. Pharmacol.* **2023**, *14*.
656 [36] B. Xiao, H. Laroui, S. Ayyadurai, E. Viennois, M. A. Charania, Y. Zhang, D. Merlin,
657 *Biomaterials* **2013**, *34*, 7471.
658 [37] Y. Zhong, B. Liang, X. Zhang, J. Li, D. Zeng, T. Huang, J. Wu, *Pulm. Circ.* **2024**,
659 *14*.
660 [38] S. Chen, S. Tang, C. Zhang, Y. Li, *Immunopharm. Immunot.* **2024**, *46*, 107.
661 [39] X. Li, X. Wu, Q. Wang, W. Xu, Q. Zhao, N. Xu, X. Hu, Z. Ye, S. Yu, J. Liu, X. He,
662 F. Shi, Q. Zhang, W. Li, *Phytomedicine* **2022**, *106*.
663 [40] Y. Liu, W. Huang, Y. Zhu, T. Zhao, F. Xiao, Y. Wang, B. Lu, *J. Agri. Food Chem.*
664 **2022**, *70*, 1148.
665 [41] B. Li, P. Du, Y. Du, D. Zhao, Y. Cai, Q. Yang, Z. Guo, *Life Sci.* **2021**, *269*.
666 [42] D. Liu, Q. Tian, K. Liu, F. Ren, G. Liu, J. Zhou, L. Yuan, Z. Fang, B. Zou, S. Wang,

667 *J. Agri. Food Chem.* **2023**, *71*, 3472.
668 [43] Z. Wu, S. Huang, T. Li, N. Li, D. Han, B. Zhang, Z. Z. Xu, S. Zhang, J. Pang, S.
669 Wang, G. Zhang, J. Zhao, J. Wang, *Microbiome* **2021**, *9*.
670 [44] A. R. Basson, A. Gomez-Nguyen, A. LaSalla, L. Butto, D. Kulpins, A. Warner, L.
671 Di Martino, G. Ponzani, A. Osme, A. Rodriguez-Palacios, F. Cominelli, *J. Nutr.*
672 **2021**, *151*, 579.
673 [45] L. Cui, X. Guan, W. Ding, Y. Luo, W. Wang, W. Bu, J. Song, X. Tan, E. Sun, Q.
674 Ning, G. Liu, X. Jia, L. Feng, *Int. J. Biol. Macromol.* **2021**, *166*, 1035.
675 [46] Y. Wu, L. Ran, Y. Yang, X. Gao, M. Peng, S. Liu, L. Sun, J. Wan, Y. Wang, K. Yang,
676 M. Yin, W. Chunyu, *Life Sci.* **2023**, *314*.
677 [47] W. Yu, X. Su, W. Chen, X. Tian, K. Zhang, G. Guo, L. Zhou, T. Zeng, B. Han,
678 *Biomed. Pharmacother.* **2019**, *113*.
679 [48] L. P. Zhao, J. Wu, W. Quan, Y. Zhou, H. Hong, G. Y. Niu, S. B. Ting-Li, S. B.
680 Huang, C. M. Qiao, W. J. Zhao, C. Cui, Y. Q. Shen, *J. Nutr. Biochem.* **2023**, *115*.
681 [49] R. Yang, Y. Wang, S. Mehmood, M. Zhao, X. Yang, Y. Li, W. Wang, J. Chen, Q.
682 Jia, *Int. J. Biol. Macromol.* **2023**, *245*.
683 [50] B. Yu, M. Wang, B. Teng, S. Veeraperumal, P. C. K. Cheung, S. Zhong, K. L.
684 Cheong, *J. Agri. Food Chem.* **2023**, *71*, 7299.
685 [51] J. Peng, X. Li, L. Zheng, L. Duan, Z. Gao, D. Hu, J. Li, X. Li, X. Shen, H. Xiao,
686 *J. Inflamm. Res.* **2022**, *15*, 1457.

Figures

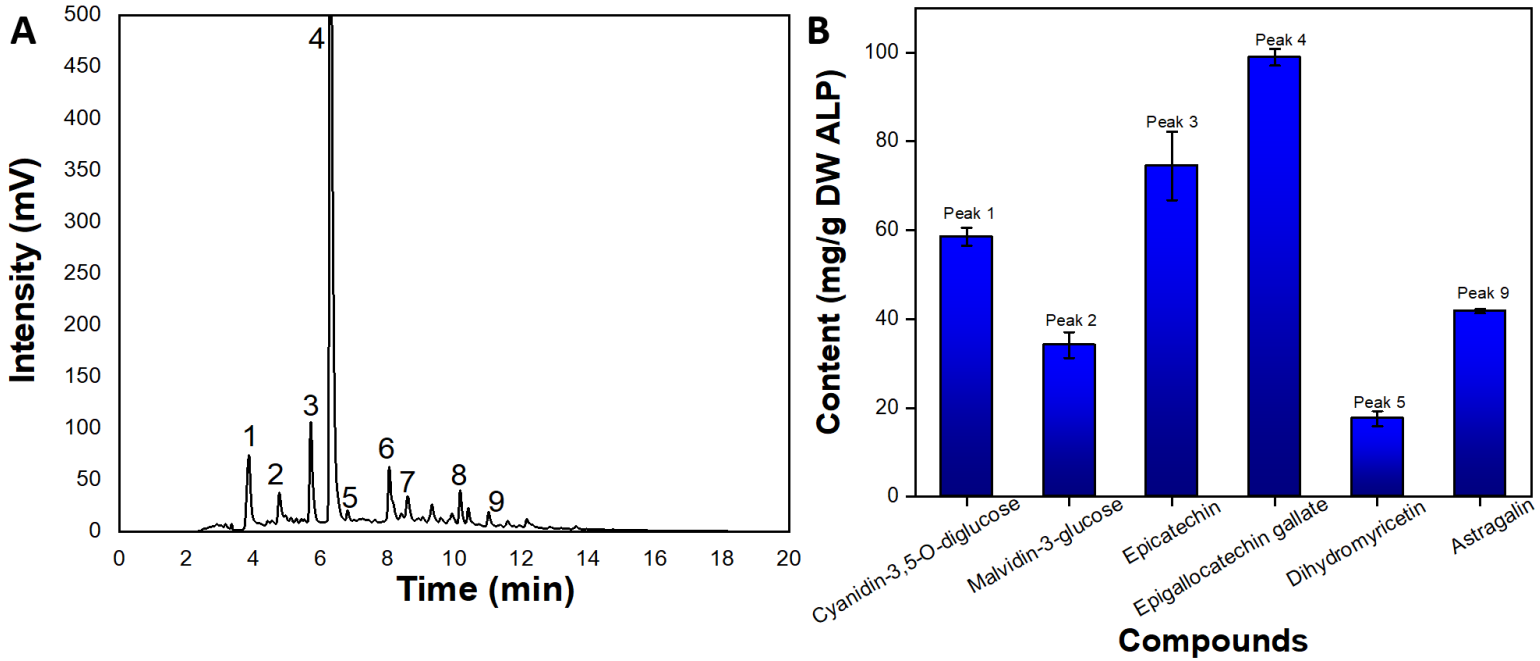

Fig. 1. HPLC-Q-Orbitrap-MS/MS profile (A) of Agarwood leaf-tea phenolics-rich extract (ALP) and the contents (B) of the major phenolic compounds identified from ALP.

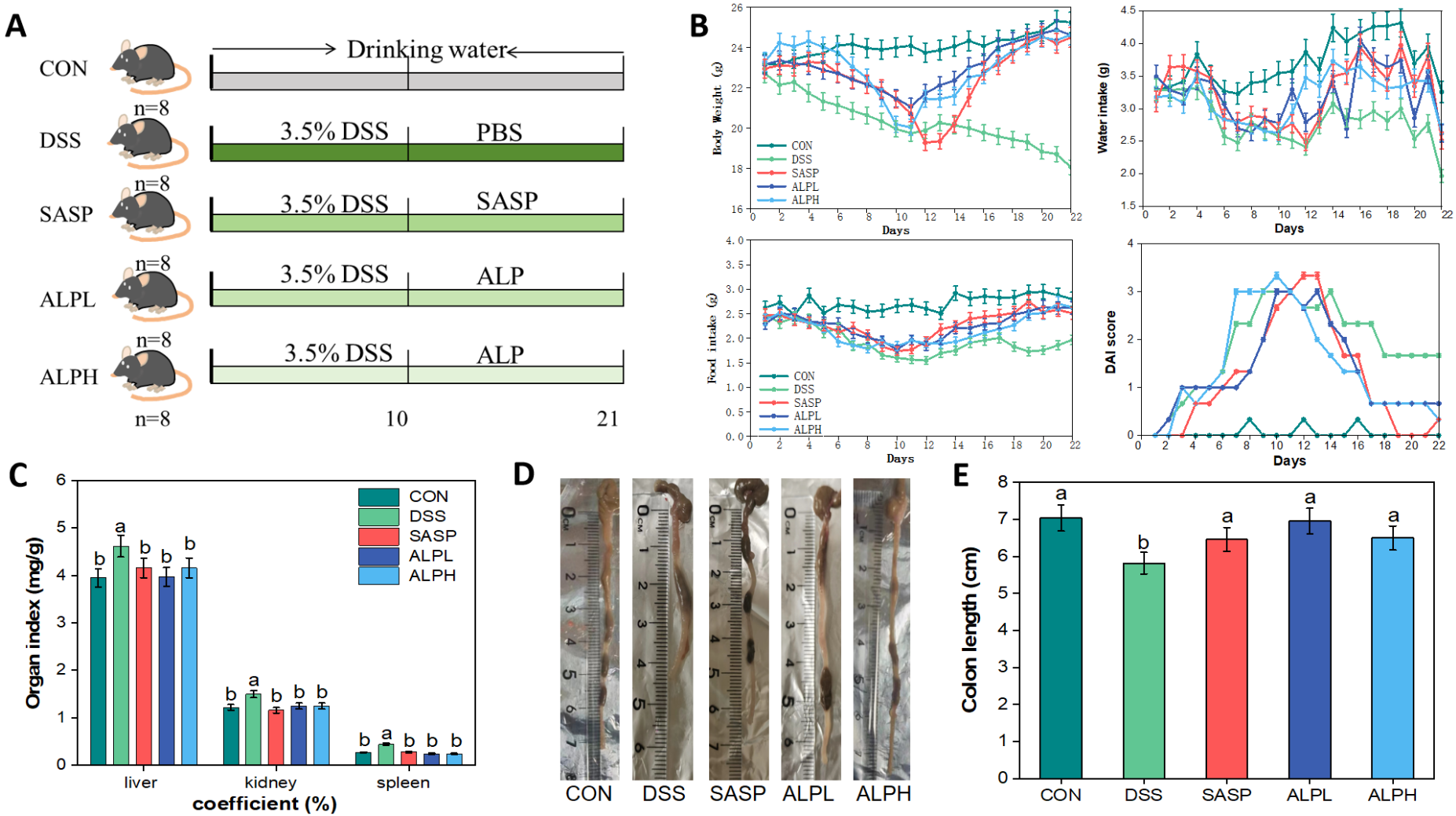
A
CON
DSS
SASP
ALPL
ALPH
n=8
Drinking water
3.5% DSS
PBS
SASP
ALP
10
21
B
Body Weight (g)
Water intake (g)
Food intake (g)
DAI score
Days
CON
DSS
SASP
ALPL
ALPH
C
Organ index (mg/g)
liver
kidney
spleen
coefficient (%)
D
E
Colon length (cm)

693

694 **Fig. 2.** Effect of ALP on basic physiological indices in a mouse model of DSS-induced ulcerative colitis. Schematic diagram of experimental
695 design (A). Water intake, food intake, body weight, and disease activity index (DAI) in mice (B). Organ index (mg/g) of mouse spleen, liver, and
696 kidney (C). Photographs of the colon (D). Colon length (cm) (E). Data are mean ± SD (n = 6). Data with different letters indicate significant
697 differences ($p < 0.05$).
698

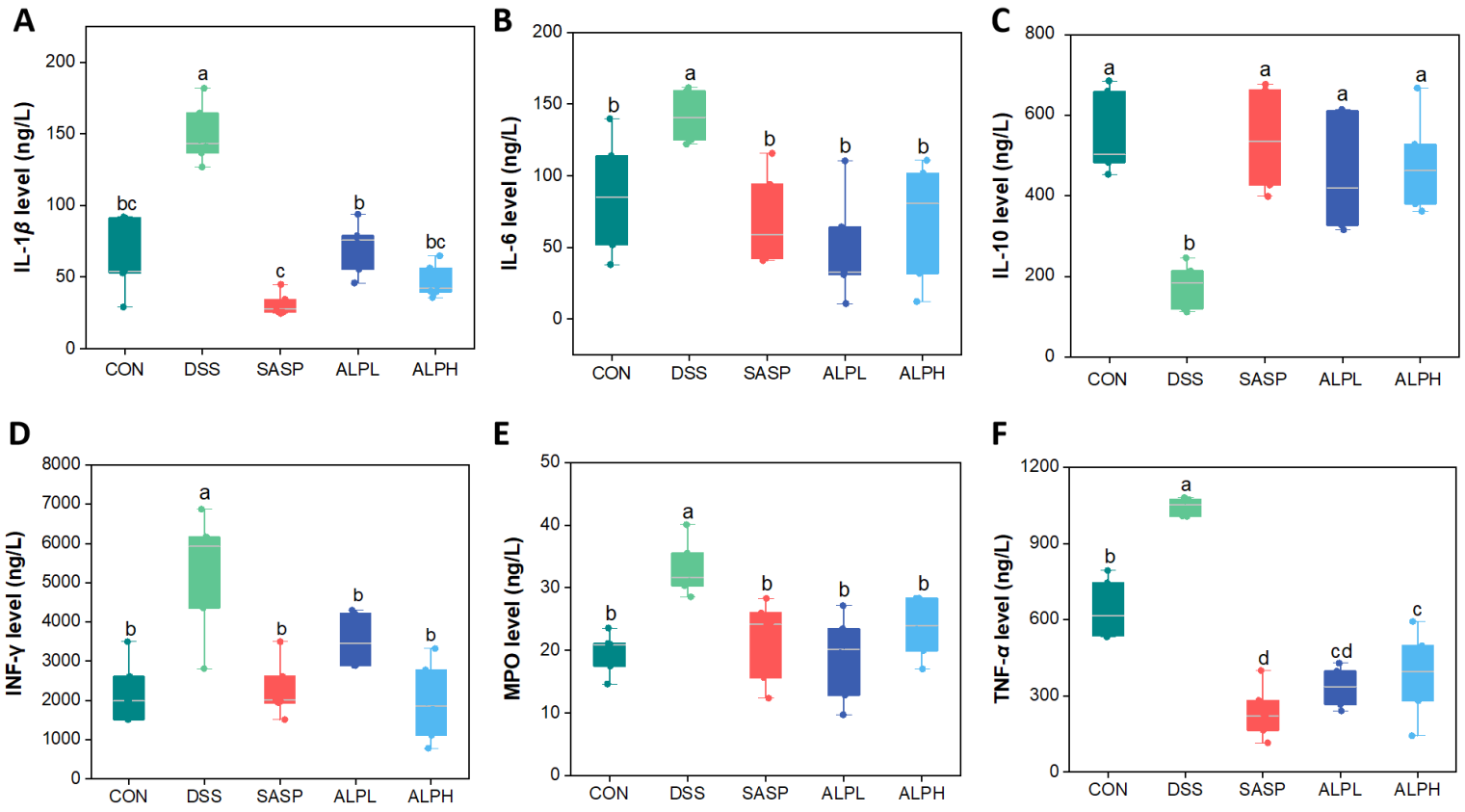

699

700 **Fig. 3.** Effect of ALP on cytokines and intestinal permeability indices in a mouse model of DSS-induced ulcerative colitis. (A) IL-1β levels. (B)

701 IL-6 levels. (C) IL-10 levels. (D) INF-γ levels. (E) MPO levels. (F) TNF-α levels. Data are mean ± SD (n = 6). Data with different letters indicate

702 significant differencest ($p < 0.05$).

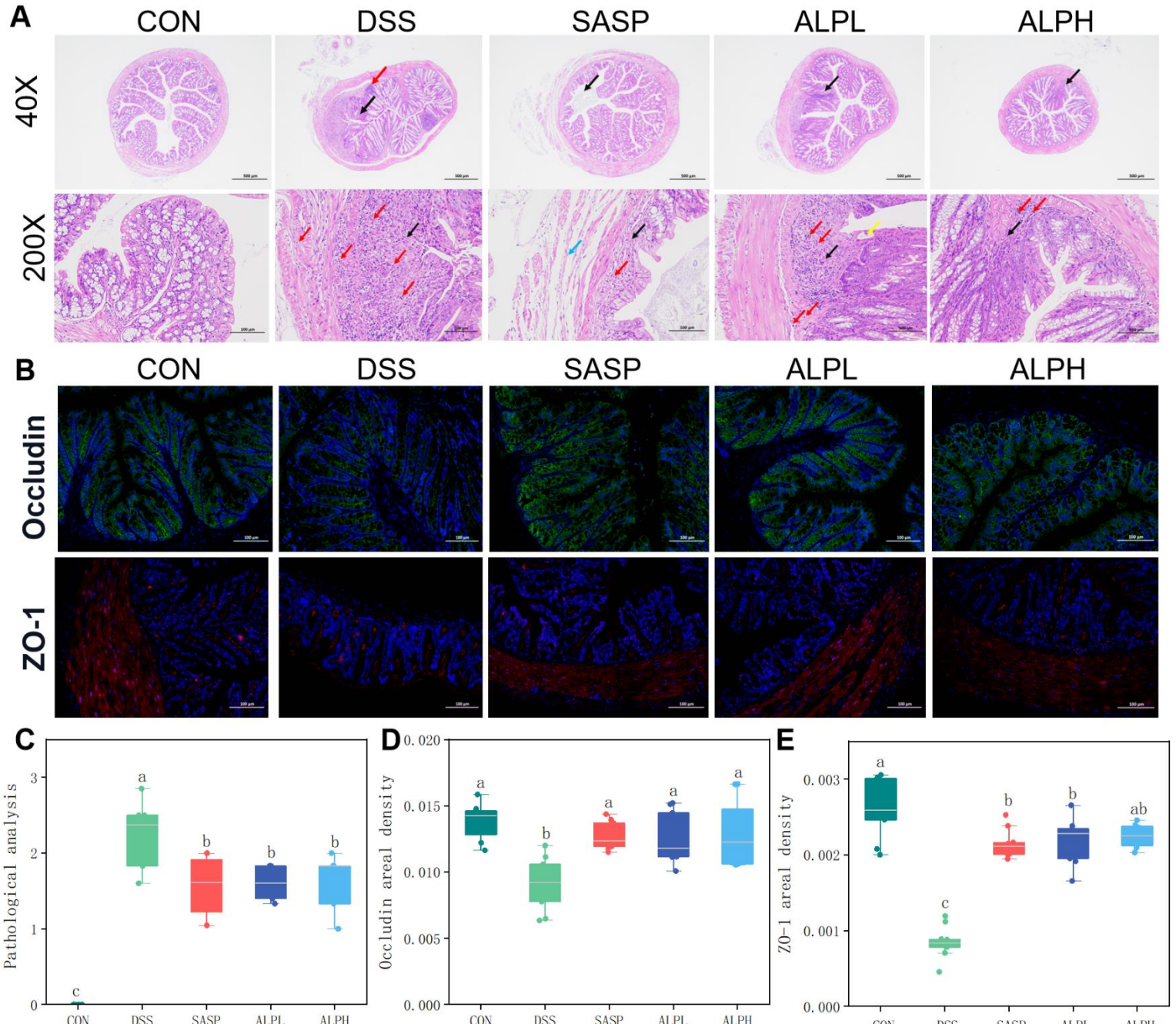
A
CON
DSS
SASP
ALPL
ALPH
40X
200X
B
CON
DSS
SASP
ALPL
ALPH
Occludin
ZO-1
C
Pathological analysis
0
1
2
3
a
b
b
b
c
CON
DSS
SASP
ALPL
ALPH
D
Occludin areal density
0.000
0.005
0.010
0.015
0.020
a
b
a
a
a
CON
DSS
SASP
ALPL
ALPH
E
ZO-1 areal density
0.000
0.001
0.002
0.003
a
c
b
b
ab
CON
DSS
SASP
ALPL
ALPH

704 **Fig. 4.** Effect of ALP on intestinal tissue morphology and tight junction-related proteins in mice with DSS-induced ulcerative colitis. Representative
705 histological observation of hematoxylin & eosin stained mouse colon at magnification of 40× and 200× (A). Immunofluorescence staining of
706 Occludin and ZO-1 (B). Histopathological scoring of colon tissue (C) Scale bar = 100 μm. Area density of Occludin immunofluorescence protein
707 (D). Area density of ZO-1 immunofluorescent protein. Red arrows indicate inflammatory cell infiltration (E); Black arrows indicate the degree of
708 ulceration; Blue arrows indicate the state of muscle distribution; Yellow arrows indicate dilated intestinal glands. Data are mean ± SD (n = 6). Data
709 with different letters indicate significant differences ($p < 0.05$).

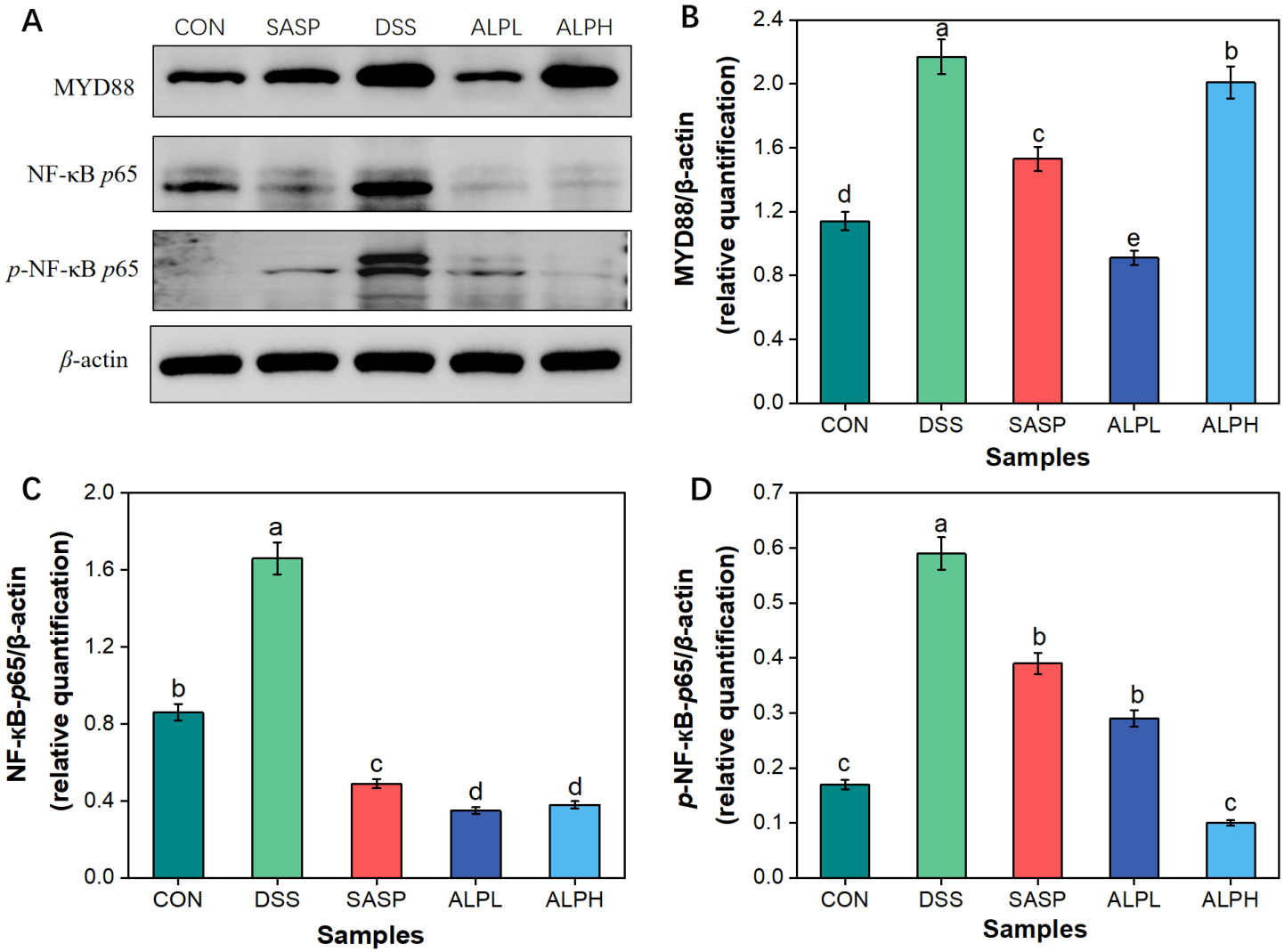
A
CON
SASP
DSS
ALPL
ALPH
MYD88
NF-κB p65
p-NF-κB p65
β-actin
B
MYD88/β-actin
(relative quantification)
Samples
C
NF-κB-p65/β-actin
(relative quantification)
Samples
D
p-NF-κB-p65/β-actin
(relative quantification)
Samples

710

711

712 **Fig. 5.** Western blot. Protein expression levels (A). MYD88 (B) NF-κB *p*65 (C) *p*-NF-κB *p*65 (D). Different lowercase letters (a-e) are used to

713 indicate significant differences between groups ($p < 0.05$).

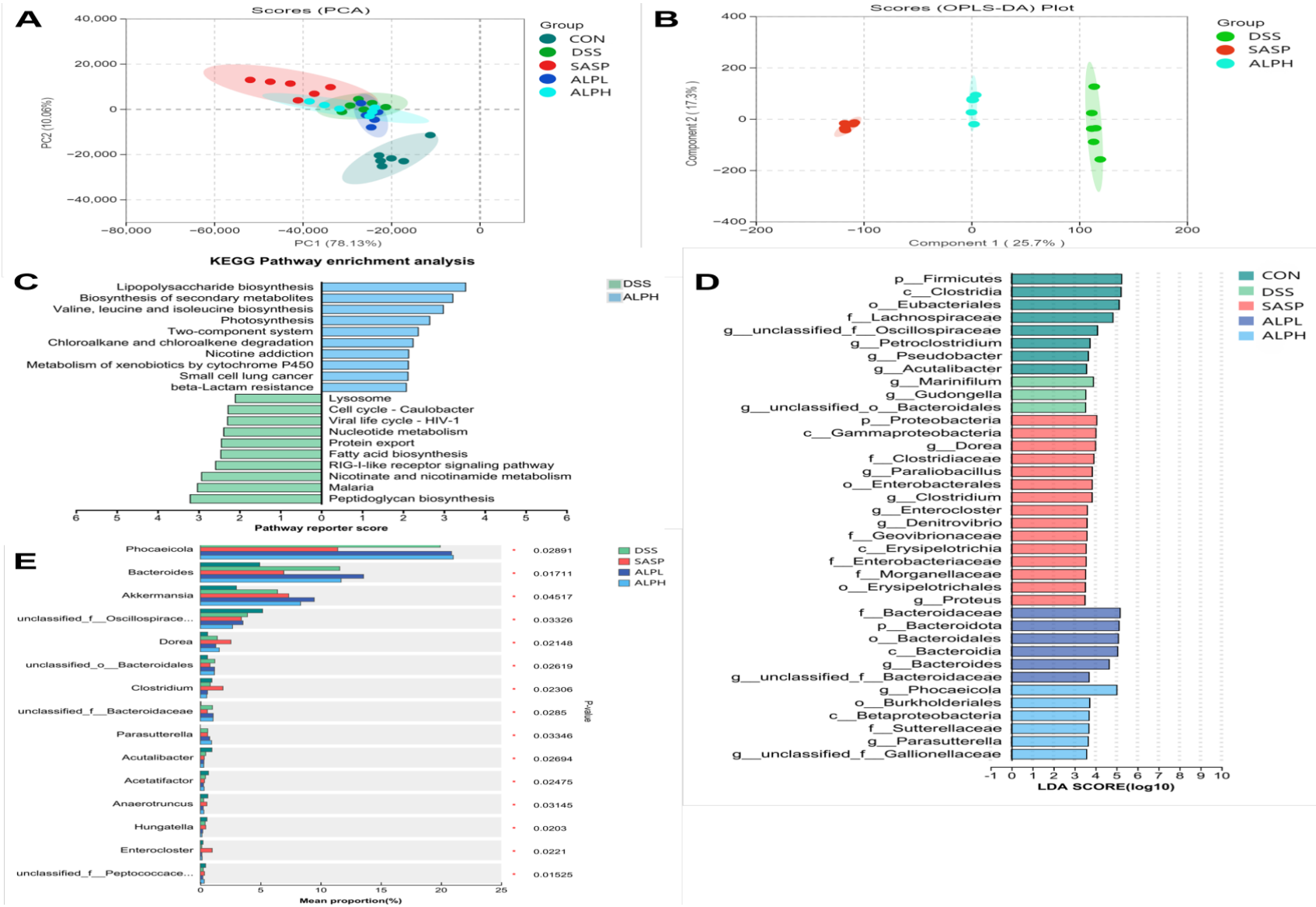
A
Scores (PCA)
Group
CON
DSS
SASP
ALPL
ALPH
PC1 (78.13%)
PC2 (10.06%)
B
Scores (OPLS-DA) Plot
Group
DSS
SASP
ALPH
Component 1 (25.7%)
Component 2 (17.3%)
C
KEGG Pathway enrichment analysis
Lipopolysaccharide biosynthesis
Biosynthesis of secondary metabolites
Valine, leucine and isoleucine biosynthesis
Photosynthesis
Two-component system
Chloroalkane and chloroalkene degradation
Nicotine addiction
Metabolism of xenobiotics by cytochrome P450
Small cell lung cancer
beta-Lactam resistance
Lysosome
Cell cycle - Caulobacter
Viral life cycle - HIV-1
Nucleotide metabolism
Protein export
Fatty acid biosynthesis
RIG-I-like receptor signaling pathway
Nicotinate and nicotinamide metabolism
Malaria
Peptidoglycan biosynthesis
DSS
ALPH
Pathway reporter score
D
p__Firmicutes
c__Clostridia
o__Eubacteriales
f__Lachnospiraceae
g__unclassified_f__Oscillospiraceae
g__Petroclostridium
g__Pseudobacter
g__Acutalibacter
g__Marinifilum
g__Gudongella
g__unclassified_o__Bacteroidales
p__Proteobacteria
c__Gammaproteobacteria
g__Dorea
f__Clostridiaceae
g__Paraliobacillus
o__Enterobacterales
g__Clostridium
g__Enterocloster
g__Denitrovibrio
f__Geovibrionaceae
c__Erysipelotrichia
f__Enterobacteriaceae
f__Morganellaceae
o__Erysipelotrichales
g__Proteus
f__Bacteroidaceae
p__Bacteroidota
o__Bacteroidales
c__Bacteroidia
g__Bacteroides
g__unclassified_f__Bacteroidaceae
g__Phocaeicola
o__Burkholderiales
c__Betaproteobacteria
f__Sutterellaceae
g__Parasutterella
g__unclassified_f__Gallionellaceae
CON
DSS
SASP
ALPL
ALPH
LDA SCORE(log10)
E
Phocaeicola
Bacteroides
Akkermansia
unclassified_f__Oscillospirace...
Dorea
unclassified_o__Bacteroidales
Clostridium
unclassified_f__Bacteroidaceae
Parasutterella
Acutalibacter
Acetatifactor
Anaerotruncus
Hungatella
Enterocloster
unclassified_f__Peptococcace...
0.02891
0.01711
0.04517
0.03326
0.02148
0.02619
0.02306
0.0285
0.03346
0.02694
0.02475
0.03145
0.0203
0.0221
0.01525
Pvalue
DSS
SASP
ALPL
ALPH
Mean proportion(%)

715 **Fig. 6.** Effect of ALP on the β-diversity of intestinal flora in mice with colitis. PCA Scores (A). OPLS-DA Scores (B). KEGG Pathway enrichment

716 analysis (C). LEfSe differential discriminant analysis (D). Significant analysis of species and functional difference (E).

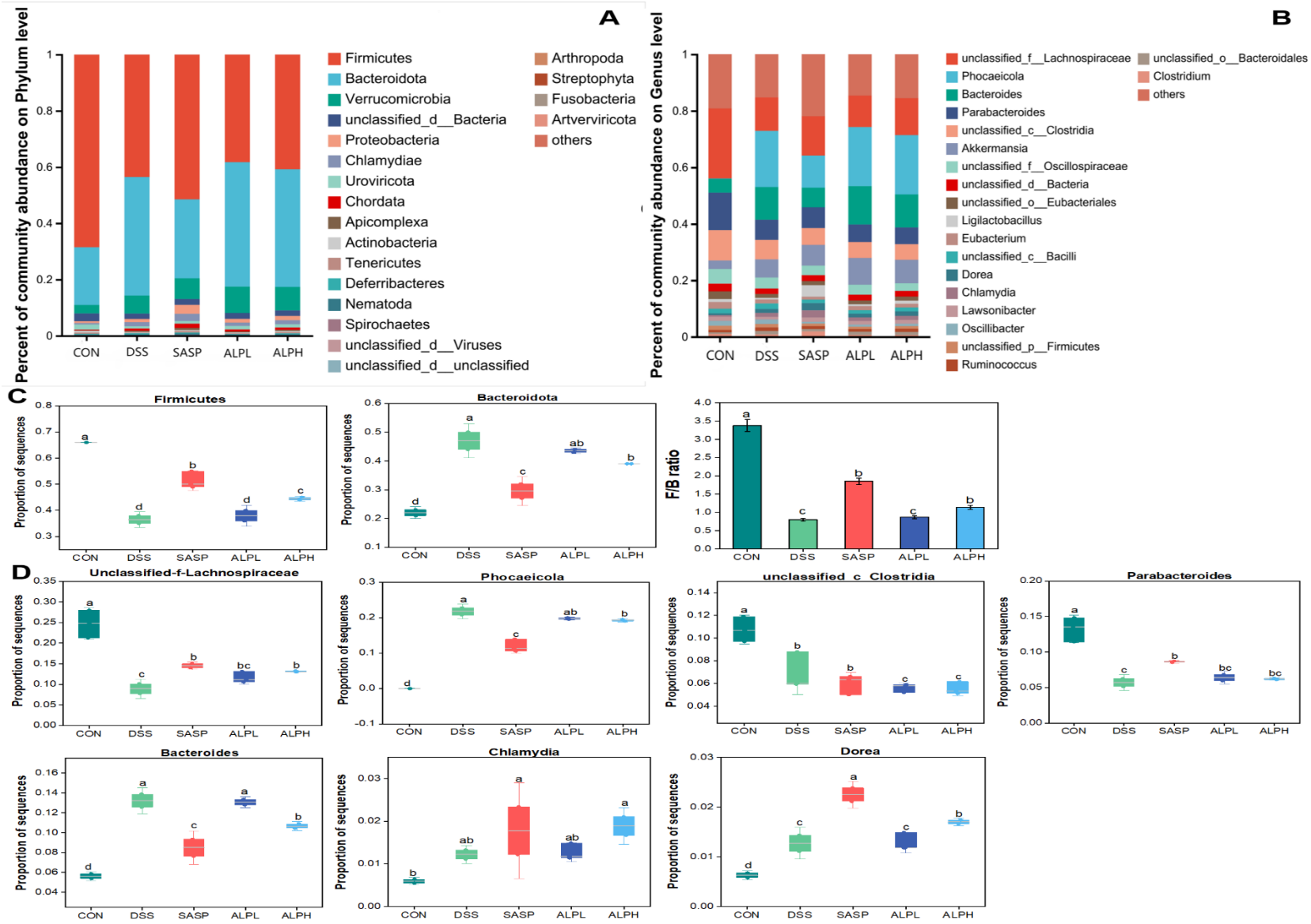
A
Percent of community abundance on Phylum level
CON
DSS
SASP
ALPL
ALPH
Firmicutes
Bacteroidota
Verrucomicrobia
unclassified_d__Bacteria
Proteobacteria
Chlamydiae
Uroviricota
Chordata
Apicomplexa
Actinobacteria
Tenericutes
Deferribacteres
Nematoda
Spirochaetes
unclassified_d__Viruses
unclassified_d__unclassified
Arthropoda
Streptophyta
Fusobacteria
Artverviricota
others
B
Percent of community abundance on Genus level
unclassified_f__Lachnospiraceae
Phocaeicola
Bacteroides
Parabacteroides
unclassified_c__Clostridia
Akkermansia
unclassified_f__Oscillospiraceae
unclassified_d__Bacteria
unclassified_o__Eubacteriales
Ligilactobacillus
Eubacterium
unclassified_c__Bacilli
Dorea
Chlamydia
Lawsonibacter
Oscillibacter
unclassified_p__Firmicutes
Ruminococcus
unclassified_o__Bacteroidales
Clostridium
others
C
Firmicutes
Bacteroidota
F/B ratio
Proportion of sequences
D
Unclassified-f-Lachnospiraceae
Phocaeicola
unclassified_c_Clostridia
Parabacteroides
Bacteroides
Chlamydia
Dorea

718 **Fig. 7.** The effect of ALP on the gut microbiota in DSS-induced ulcerative colitis mouse models. Species composition of intestinal flora at the
719 phylum level (A). Species composition of intestinal flora at the genus level (B). Main microbial communities at the phylum level. (D) Main
720 microbial communities at the genus level (C) ($p < 0.05$).
721

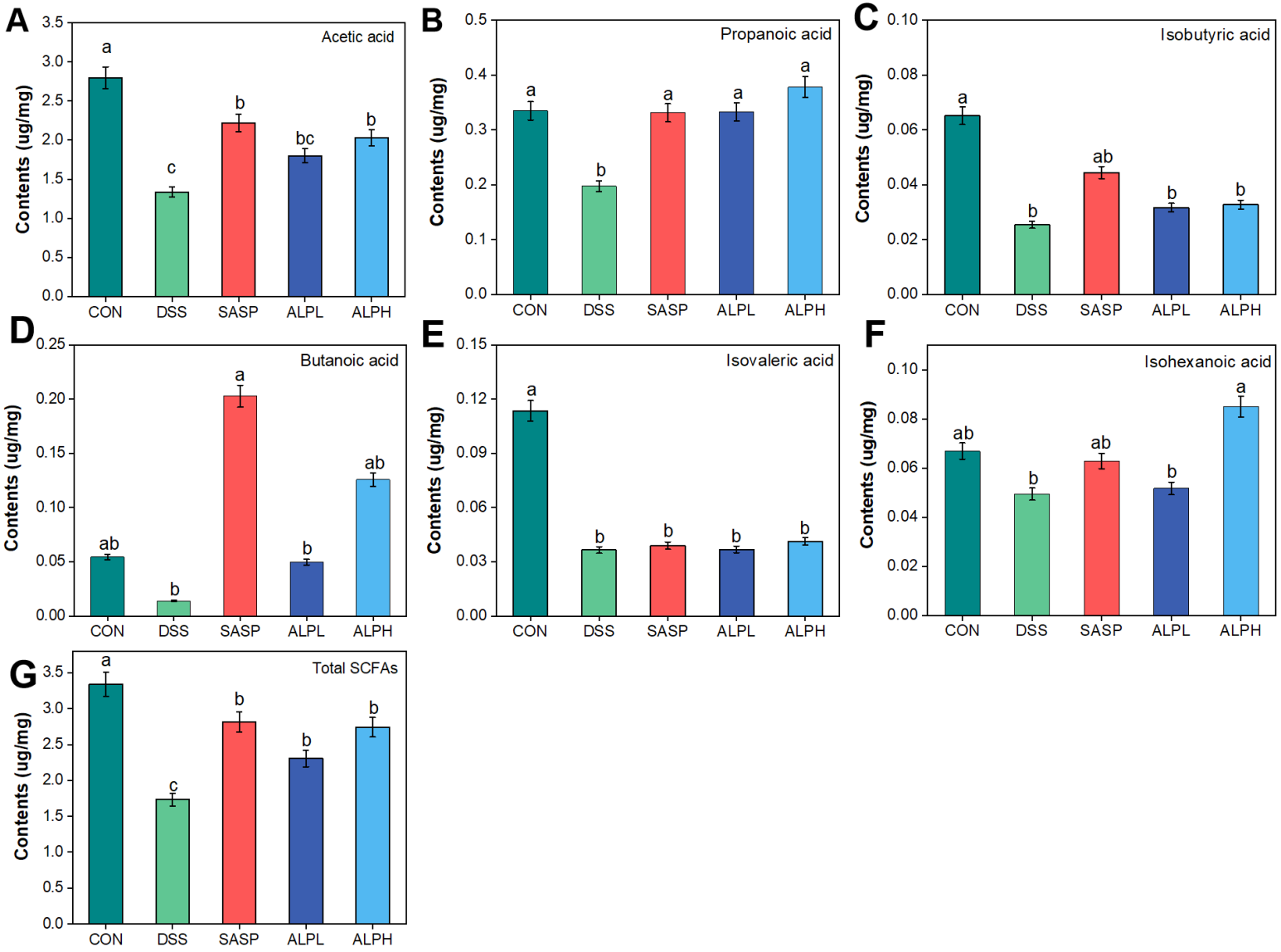
A
Acetic acid
Contents (ug/mg)
a
c
b
bc
b
B
Propanoic acid
Contents (ug/mg)
a
b
a
a
a
C
Isobutyric acid
Contents (ug/mg)
a
b
ab
b
b
D
Butanoic acid
Contents (ug/mg)
ab
b
a
b
ab
E
Isovaleric acid
Contents (ug/mg)
a
b
b
b
b
F
Isohexanoic acid
Contents (ug/mg)
ab
b
ab
b
a
G
Total SCFAs
Contents (ug/mg)
a
c
b
b
b
CON
DSS
SASP
ALPL
ALPH

722

723 **Fig. 8.** Effect of ALP on the levels of SCFAs in a mouse model of DSS-induced ulcerative colitis: Acetic acid (A); Propanoic acid (B); Isobutyric
724 acid (C); Butanoic acid (D); Isovaleric acid (E); Isohexanoic acid (F) and total SCFAs (G). Data are mean ± SD (n = 6). Data with different letters
725 indicate significant differences ($p < 0.05$).
726

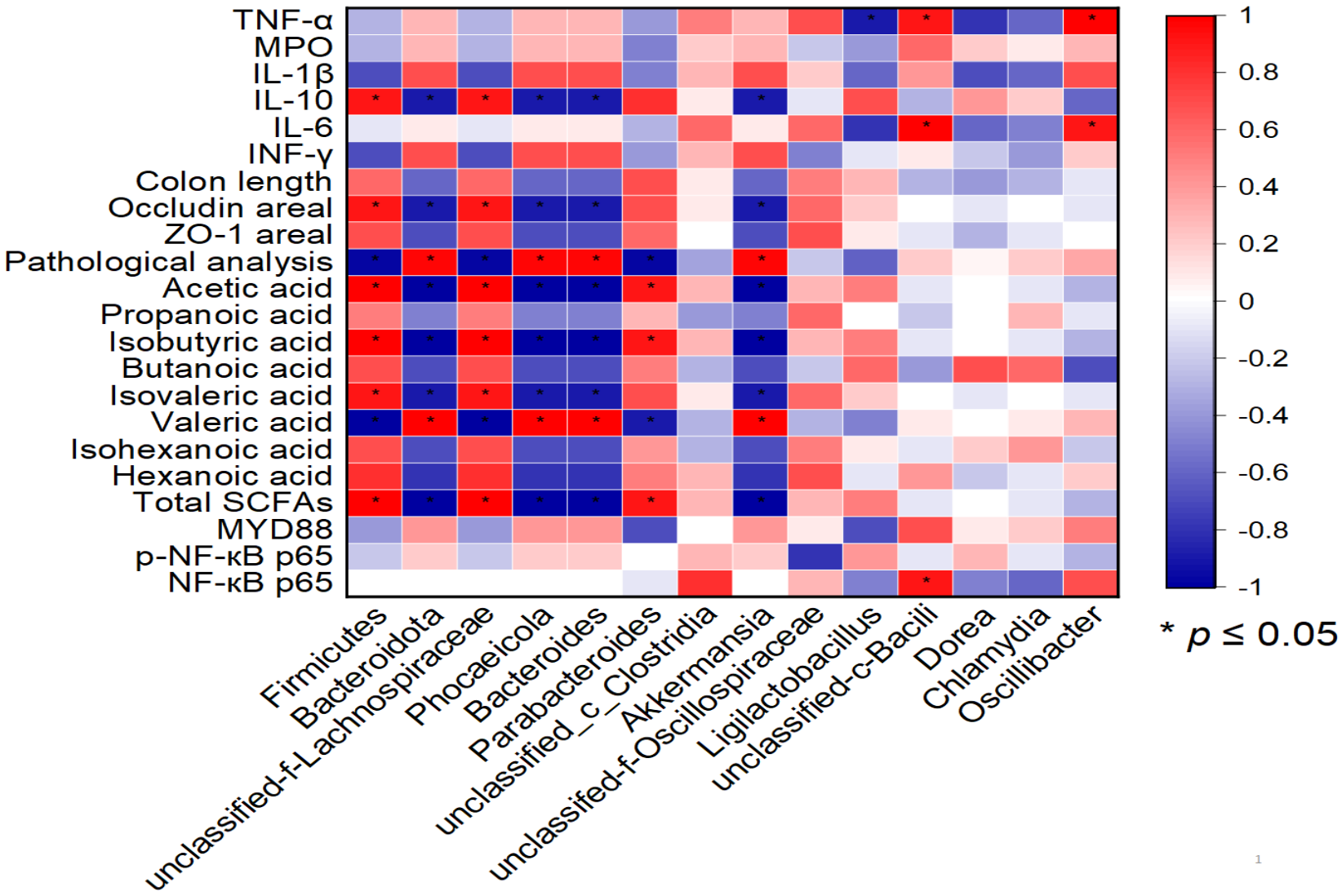
TNF-α
MPO
IL-1β
IL-10
IL-6
INF-γ
Colon length
Occludin areal
ZO-1 areal
Pathological analysis
Acetic acid
Propanoic acid
Isobutyric acid
Butanoic acid
Isovaleric acid
Valeric acid
Isohexanoic acid
Hexanoic acid
Total SCFAs
MYD88
p-NF-κB p65
NF-κB p65
Firmicutes
Bacteroidota
unclassified-f-Lachnospiraceae
Phocaeicola
Bacteroides
Parabacteroides
unclassified_c_Clostridia
Akkermansia
unclassified-f-Oscillospiraceae
Ligilactobacillus
unclassified-c-Bacili
Dorea
Chlamydia
Oscillibacter
1
0.8
0.6
0.4
0.2
0
-0.2
-0.4
-0.6
-0.8
-1
* p ≤ 0.05

727

728 **Fig. 9.** Correlation between gut microbiota and biochemical indicators associated with DSS-induced ulcerative colitis (* $p \leq 0.05$).

729